Visual Neuroscience (1990), **5**, 43–60. Printed in the USA.

A burst of differentiation in the outer posterior retina of the eleven-week human fetus: An ultrastructural study

KENNETH A. LINBERG[1] AND STEVEN K. FISHER[2]

[1]Neuroscience Research Institute, University of California, Santa Barbara
[2]Neuroscience Research Institute and Department of Biological Sciences, University of California, Santa Barbara

(RECEIVED January 2, 1990; ACCEPTED March 28, 1990)

Abstract

Many studies on human retinal development have cited the third gestational month as a period when the posterior retina undergoes rapid differentiation and maturation, including a lining up of cone precursors. Ultrastructural data on the posterior retina during the third month are very limited, and totally lacking for the cone monolayer. We have examined two human fetal retinas between ten and 11 gestational weeks. Before the appearance of the cone monolayer, the outer neural retina consists of a homogeneous population of undifferentiated neuroblasts. Mitotic figures are still evident, even posteriorally. There is no outer plexiform layer (OPL). The interface of neural retina to retinal pigment epithelium (RPE) is largely featureless. By 11 weeks, the posterior retina has a thin OPL that separates the many rows of cells in the developing inner nuclear layer from the single tier of macular cone precursors. The RPE monolayer consists of cuboidal cells whose apical surface elaborates ridges of cytoplasm and branched processes that project into the subretinal space. The large, cuboidal cones are linked to each other and Müller cells at the outer limiting membrane. They show definitive signs of the structural polarity typical of vertebrate photoreceptors. Their apical cytoplasm contains many organelles common to the inner segment, while the basal cytoplasm has synaptic ribbons and vesicles, and receives invaginating contacts from processes in the OPL neuropil arising from differentiating second-order neurons. Lateral cone surfaces are mutually underlain by large subsurface cisterns.

Keywords: Photoreceptor, Electron microscopy, Development, Macular cones, Outer nuclear layer

Introduction

The prenatal development of the human retina has been well-documented by light microscopy (Barber, 1955; Hervouët, 1958; Duke-Elder & Cook, 1963; O'Rahilly, 1966, 1975; Mann, 1969; Rhodes, 1979; Provis et al., 1985). Corresponding ultrastructural data are limited to the three surveys of Yamada and Ishikawa (1965) and Hollenberg and Spira (1972, 1973) encompassing the period from $6\frac{1}{2}$ weeks of embryonic life to term, and the more specialized studies focused on specific cell types, retinal regions, or developmental stages (Fisher & Linberg, 1975; Mund & Rodrigues, 1979; Rhodes, 1984; Johnson et al., 1985).

Hollenberg and Spira (1972, 1973) described developing cones in the 12-week [83 mm crown-rump length (CR)] fetal retina, although numerous light-microscopic studies indicate that the cones first appear as a recognizable monolayer in the posterior pole of the eye a week or more earlier (65–71 mm) (Barber, 1955; Hervouët, 1958; Duke-Elder & Cook, 1963; Rhodes, 1979). In studying two well-preserved human fetal retinas, we found that the retina of the 55-mm specimen lacked such a monolayer, while that of the 61-mm specimen had a small, but definite monolayer of cone precursors at its posterior pole. These have not been previously described by electron microscopy. Our results show that as these cells begin to differentiate, they interact with emerging processes from the apical RPE, establish their characteristic cytoplasmic polarity, and form synaptic contact with processes in the primitive OPL neuropil emanating from differentiating second-order neurons.

Reprint requests to: Steven K. Fisher, Neuroscience Research Institute, University of California, Santa Barbara, CA 93106, USA.

Material and methods

Retinas from two human fetuses obtained at the time of hysterectomy were studied by light and electron microscopy. These fetuses had crown-rump lengths of 55 mm and 61 mm [about 10–11 weeks of age according to the growth curves of Patten (1953)]. Eyes were enucleated within 15 min of surgery. A small equatorial slit was made in each globe immediately before immersion in 2.5% glutaraldehyde in 0.067 M sodium cacodylate buffer at pH 7.3 and 20°C. Within 30 min, the anterior portion of each eye was removed and the posterior portion was re-

immersed in cold (4°C) fixative for an additional 2–3 h. The specimens were then rinsed in two 1-h changes of isotonic buffer (45 mg/ml sucrose added) prior to postfixation in 2% OsO_4 in 0.1 M veronal acetate buffer for an additional 1 $\frac{1}{2}$ h at 4°C. Following several rinses in distilled water, the tissue was dehydrated in ethanol, transferred to propylene oxide, infiltrated, and embedded in Araldite 6005.

One-micron semi-thick sections, stained with toluidine blue, were studied and photographed on a Zeiss Photomicroscope III (Thornwood, NJ). For electron microscopy, thin sections were mounted on copper-mesh grids except for the serial thin sections which were placed on formvar-coated slot grids. All sections were stained with 1% uranyl acetate (or a 1:1 ratio of saturated, aqueous uranyl acetate to absolute methanol), followed by Reynold's lead citrate. Sections were examined by transmission electron microscopy.

Results

Figure 1 shows by light microscopy the major cellular transformations occurring in the outer posterior retina between the 55-mm and 61-mm specimens. The examples shown represent the most advanced state of morphological differentiation found in each specimen. At 61-mm, the eyecup had a diameter of 4.5 mm. Based on the composite of our observations by both light and electron microscopy, the retina can be divided into four roughly concentric zones. The central, differentiated zone (Fig. 1B) is about 750 μm in diameter and offset slightly from the center of the posterior pole. The outer retina of this region consists of a uniform lineup of cone precursors, underlain by a narrow outer plexiform layer (OPL). Surrounding this zone is a strip of retina 400–600 μm wide, wherein the emerging OPL can still be discerned but with less-differentiated cones. Encircling this zone lies another band of retina 850–1500 μm wide that lacks an OPL. The largest and most peripheral zone has many mitotic figures lying among the neuroblasts. Mitotic figures were not found in the inner three zones.

The retinal pigment epithelium

In both specimens, the developing retinal pigment epithelium (RPE) is a monolayer about 7 μm deep (Figs. 1–4) underlain by a 60–70-nm-thick basement membrane and a partially differentiated Bruch's membrane (0.75–1.0 μm thick). The basal membrane of the RPE is smooth except for baso-lateral infoldings. Apically, these cells are joined by prominent junctional complexes (Figs. 3 and 4). RPE cell nuclei lie in mid-cytoplasm surrounded by numerous melanosomes, their precursors, and other organelles (Figs. 2–4). No mitotic figures were observed in the RPE of either specimen.

One major difference in RPE morphology between the two specimens is the increased complexity of the apical surface at 61 mm which in profile appears scalloped (Fig. 1B), and which elaborates large and complex apical processes into the expanded subretinal space (SRS) (Figs. 3, 4, 5A, and 5B). Apical RPE cytoplasm extends down into wedge-shaped, organelle-rich "ridges" forming cup-shaped profiles over the differentiating cones (Figs. 3, 4, 5A, and 6A). The apex of each ridge usually opposes the outer Müller processes (Figs. 3, 4, 5A, 6A, 7, and 8) that are interposed between cone precursors. RPE ridges often contain prominent stacks of rough endoplasmic reticulum (RER) (Figs. 3, 5A, and 6A) not common in the younger specimen. Most apical RPE processes are thin, unbranched and have an actin core. Although not numerous, they can arise from any point on the apical RPE surface. The more complex, branching processes usually emanate from the apical ridges (Figs. 3, 5A, 5B, 6A, and 8) and project into the SRS where they intermingle with microvilli from both Müller cells and cone precursors (Figs. 3, 5A, 5B, 7, and 8). Paired centrioles often lie near the apical surface (Figs. 3 and 6A). Sometimes one centri-

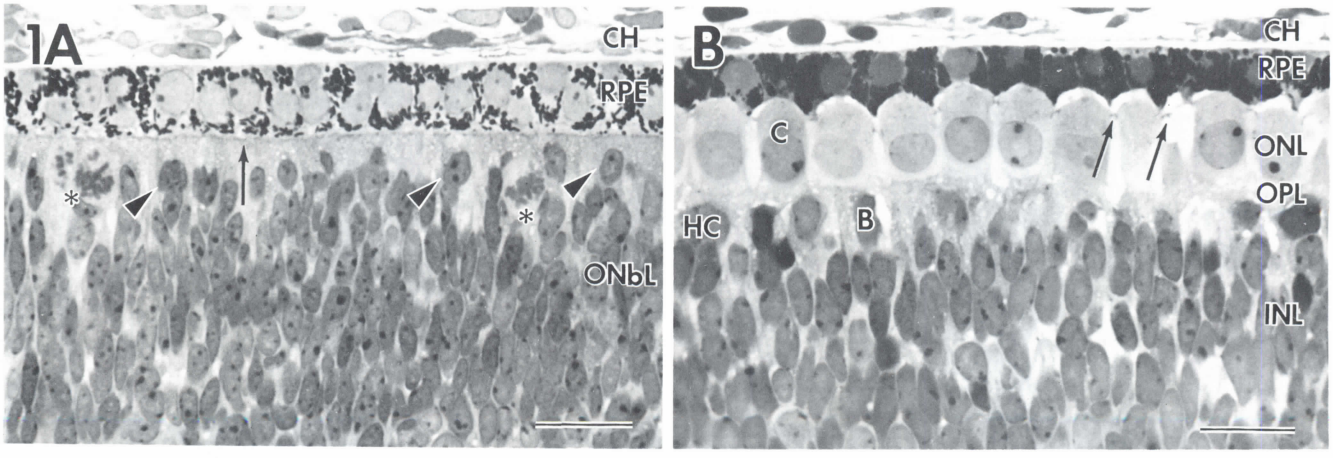

Fig. 1. Light micrographs of 1-μm sections of human fetal retina, stained by toluidine blue. A: The retinal-RPE interface near the posterior pole of the 55-mm human fetus. The two cell layers are closely apposed. The outer limiting membrane (OLM) (arrow) appears largely uninterrupted along this interface. Several retinal cells along the SRS have rounded nuclei (arrowheads), while those deeper in the outer neuroblast layer (ONbL) are oval. Note the mitotic figures (*). No OPL is seen. CH: choroid. B: A similar retinal area in the 61-mm human fetus. A single layer of rectangular cone precursors (C) constitutes the primitive ONL. Their lightly staining cytoplasm contrasts with that of the RPE and of the cells in the INL. Apical cone cytoplasm bulges beyond the OLM (arrows). A narrow OPL separates the layer of cones from cells of the INL. Horizontal (HC) and bipolar cells (B) at the outer edge of the INL are also differentiating. Scale bars = 10 μm.

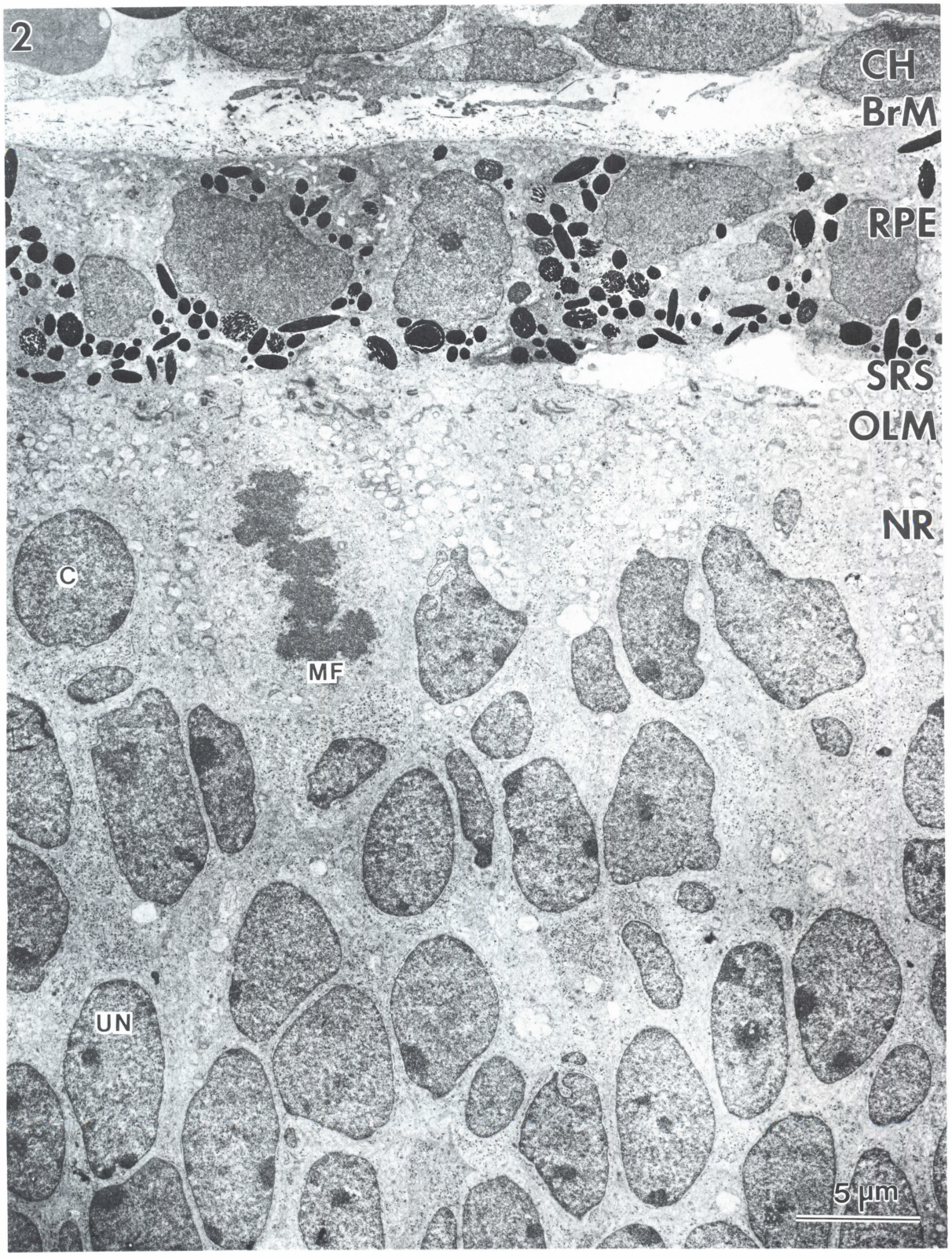

Fig. 2. The outer posterior retina and RPE at 55 mm. A developing Bruch's membrane (BrM) separates the RPE monolayer from the endothelial cells of the choriocapillaris (CH). In most places, the retinal pigment epithelium (RPE) directly apposes the cells of the neural retina (NR), but at the right, a narrow subretinal space (SRS) separates the two layers. The outermost row of the neural retina includes a mitotic figure (MF) and cells with rounded or indented nuclei (C) lying above rows of oval nuclei typical of undifferentiated cells (UN) deeper in the outer neuroblast layer. No outer plexiform layer (OPL) is evident. OLM: outer limiting membrane. Scale bar = 5 μm.

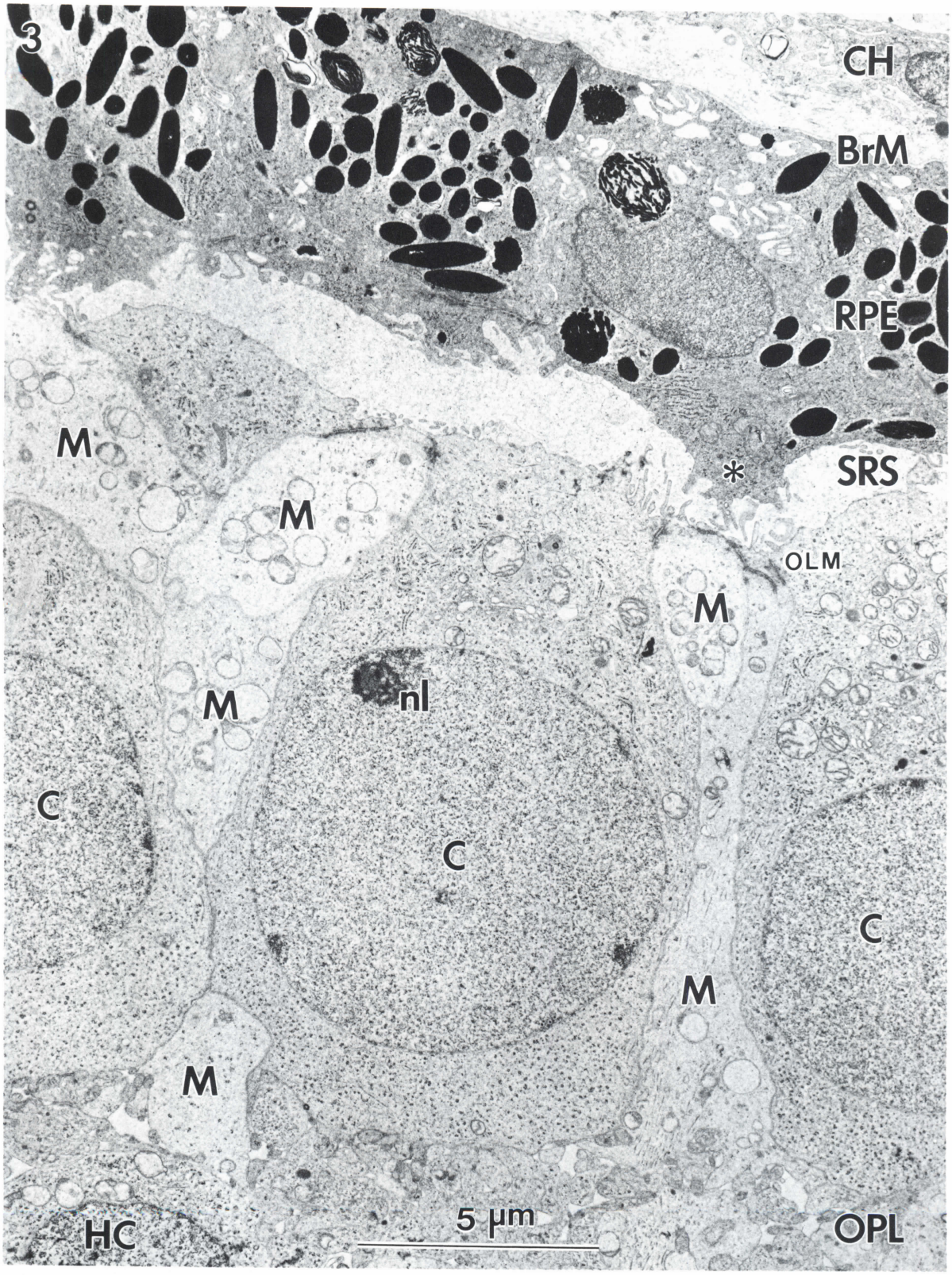

Fig. 3. At 61 mm, the posterior RPE is a true monolayer. A ridge of cytoplasm (*) projects from the RPE towards the neural retina. An expanded subretinal space (SRS), here about 1.5 μm wide, contains villous processes from the cells of both layers. Cone precursors (C), with spherical nuclei and swollen apical cytoplasm, are easily distinguishable from the more electron-lucent Müller cell (M) processes that separate them at the outer limiting membrane (OLM). A narrow outer plexiform layer (OPL) lies between the cone precursors and second-order neurons, including a horizontal cell (HC). CH: choroid; BrM: Bruch's membrane; nl: nucleolus. Scale bar = 5 μm.

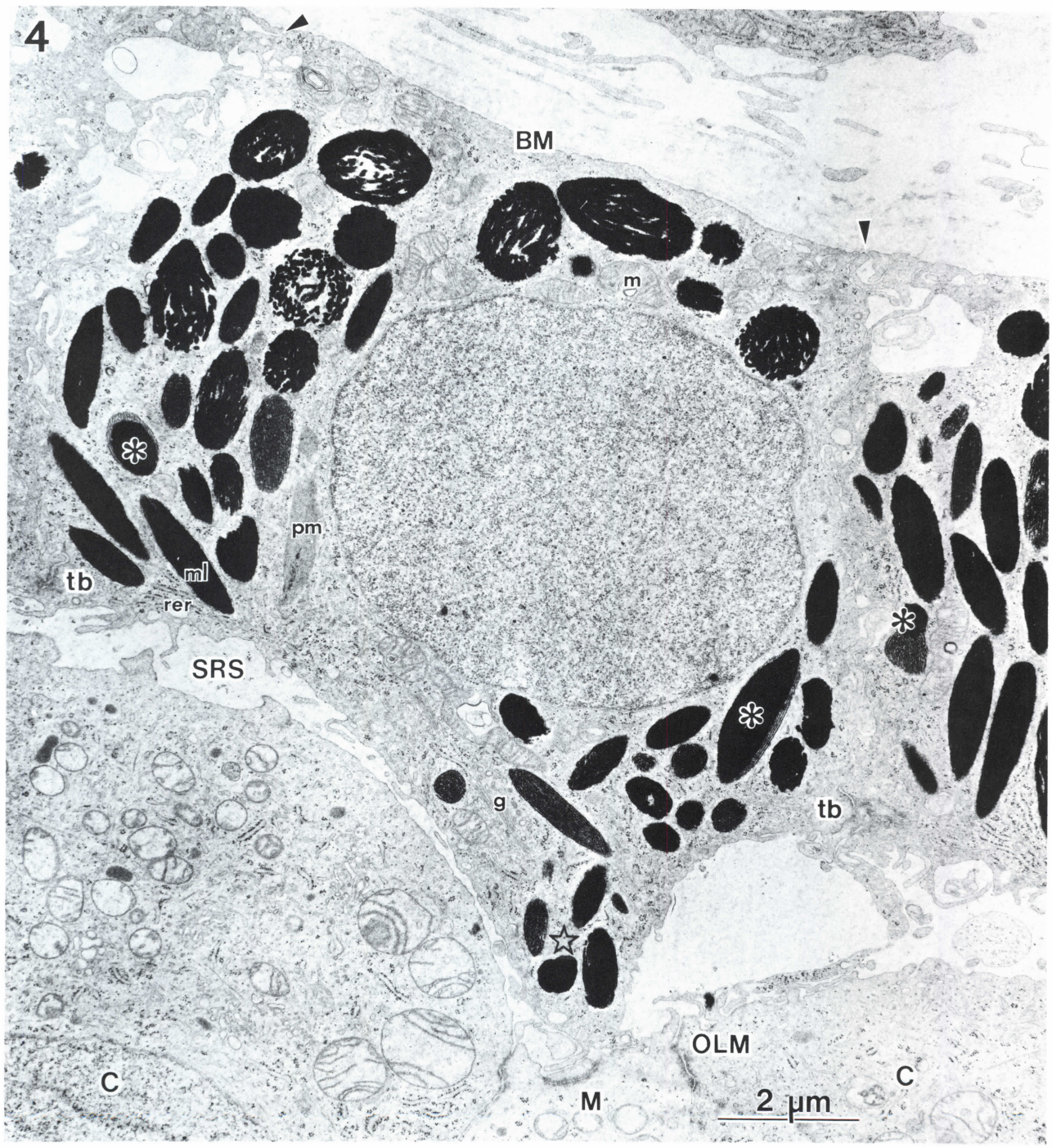

Fig. 4. An RPE cell in the posterior pole at 61 mm. Basement membrane (BM) lines its basal surface. Arrowheads indicate basolateral infoldings. A junctional complex (tb) joins the cells' apico-lateral surfaces. The rounded nucleus is surrounded by many melanosomes (ml) and premelanosomes (pm). Spindle-shaped melanin profiles predominate. Certain premelanosomes show two different stages of melanin deposition (*). At the left, small villous processes project into the subretinal space (SRS), while at the right, an organelle-rich ridge of RPE cytoplasm (star) extends across the SRS to closely contour the membrane of a cone precursor (C), and end closely apposed to a Müller cell process (M). The apical cytoplasm of the cone precursor on the left contains many organelles and bulges beyond the outer limiting membrane (OLM). g: Golgi body; m: mitochondrion; rer: rough endoplasmic reticulum. Scale bar = 2 μm.

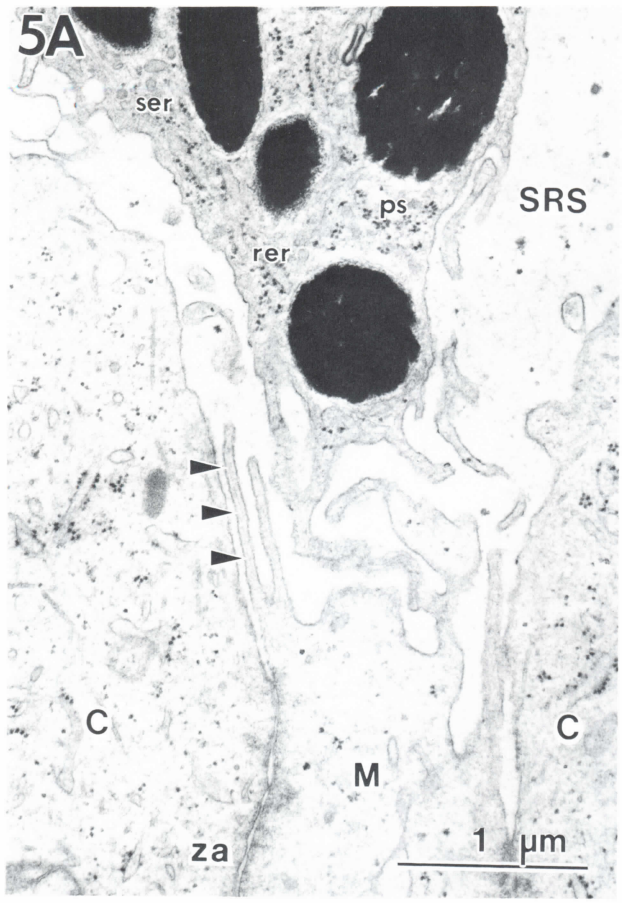

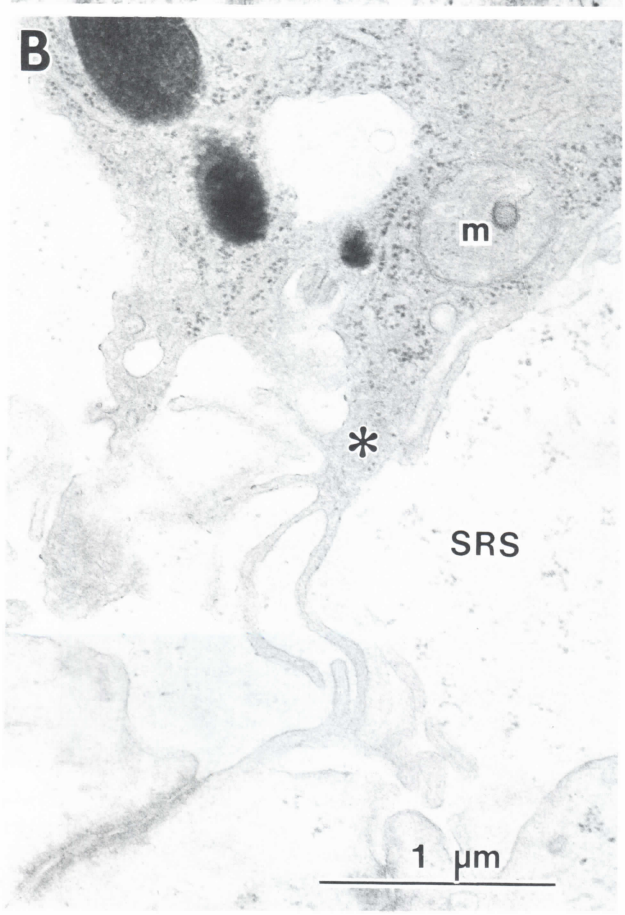

ole serves as a basal body to a cilium protruding into the SRS (Fig. 6B).

The cone precursors

By electron microscopy, the thick layer of cells constituting the outer posterior retina at 55 mm (Fig. 2) appear largely undifferentiated. Adhering junctions between neural retinal cells form an outer limiting membrane (OLM) along the outer border of the retina. Cells with rounded nuclei are often seen here (Figs. 1A and 2). They overlie numerous ranks of undifferentiated cells whose oval perikarya lie deeper in the outer neuroblast layer. Mitotic figures also appear regularly along this border, intermixed with the more rounded cells (Figs. 1A and 2). Dividing cells retain their junctional complexes at the OLM. The rounded cells show some partitioning of organelles with the greatest number and variety lying in the apical cytoplasm (Fig. 2). Neither synaptic vesicles nor synaptic ribbons have been observed in them. The outer processes of Müller cells cannot yet be identified at the OLM. There is no OPL.

At the posterior pole of the 61-mm specimen, the neural retina is divided into distinct layers by a thick inner plexiform layer (IPL) and a narrow, sometimes discontinuous OPL. A monolayer of differentiating cones with pale cytoplasm and distinctively round nuclei contrasts with the rows of darkly staining, oval perikarya of cells lying beneath it (Fig. 1B). Cone cytoplasm is now markedly polarized; these cells are rectangular in profile, averaging 10 μm wide by 16 μm deep. Their nuclei, usually just over 8 μm in diameter, are displaced slightly towards the OPL (Figs. 1B, 3, and 7) and often have two nucleoli.

The apical cone cytoplasm

One distinguishing feature of the developing cone at 61 mm is the extension of its apical cytoplasm beyond the OLM into the SRS (Figs. 6B, 8, and 9). These extensions are free of organelles except for ribosomes and agranular cisternae that lie in a fine ground substance. They sometimes connect to the rest of the apical cone cytoplasm by a narrow neck, although most often the two regions are broadly continuous (Figs. 8 and 9). A pair of centrioles, the precursors of basal bodies to the outer segment cilia, lie among the cytoplasmic organelles well beneath these extensions, never close to the cell surface (Fig. 9). Often ciliary rootlets (periodicity 80 nm) and microtubules extend from them.

The inner portion of the apical cytoplasm, the future myoid, is richly populated with mitochondria, RER, and Golgi bodies associated with 60–70 nm vesicles (Figs. 3,4, and 7–9). Lysosomes occur throughout the cell, except for the apical outgrowth, but are found in the greatest density here (Figs. 7–9) often clustering near presumed autophagic vacuoles. Cisternae

Fig. 5. Posterior retina; 61 mm. A: An RPE ridge contains mature melanosomes, rer, ser, and polysomes (ps). It elaborates apical processes across the subretinal space (SRS) that intermingle with Müller-cell (M) apical microvilli. The microfilamentous core of one process is visible (arrowheads). C: cone precursor; za: zonula adhaerens. rer: rough endoplasmic reticulum; ser: smooth endoplasmic reticulum. Scale bar = 1 μm. B: Another RPE ridge elaborates an array of villous processes radiating (*) into the SRS. m: mitochondrion. Scale bar = 1 μm.

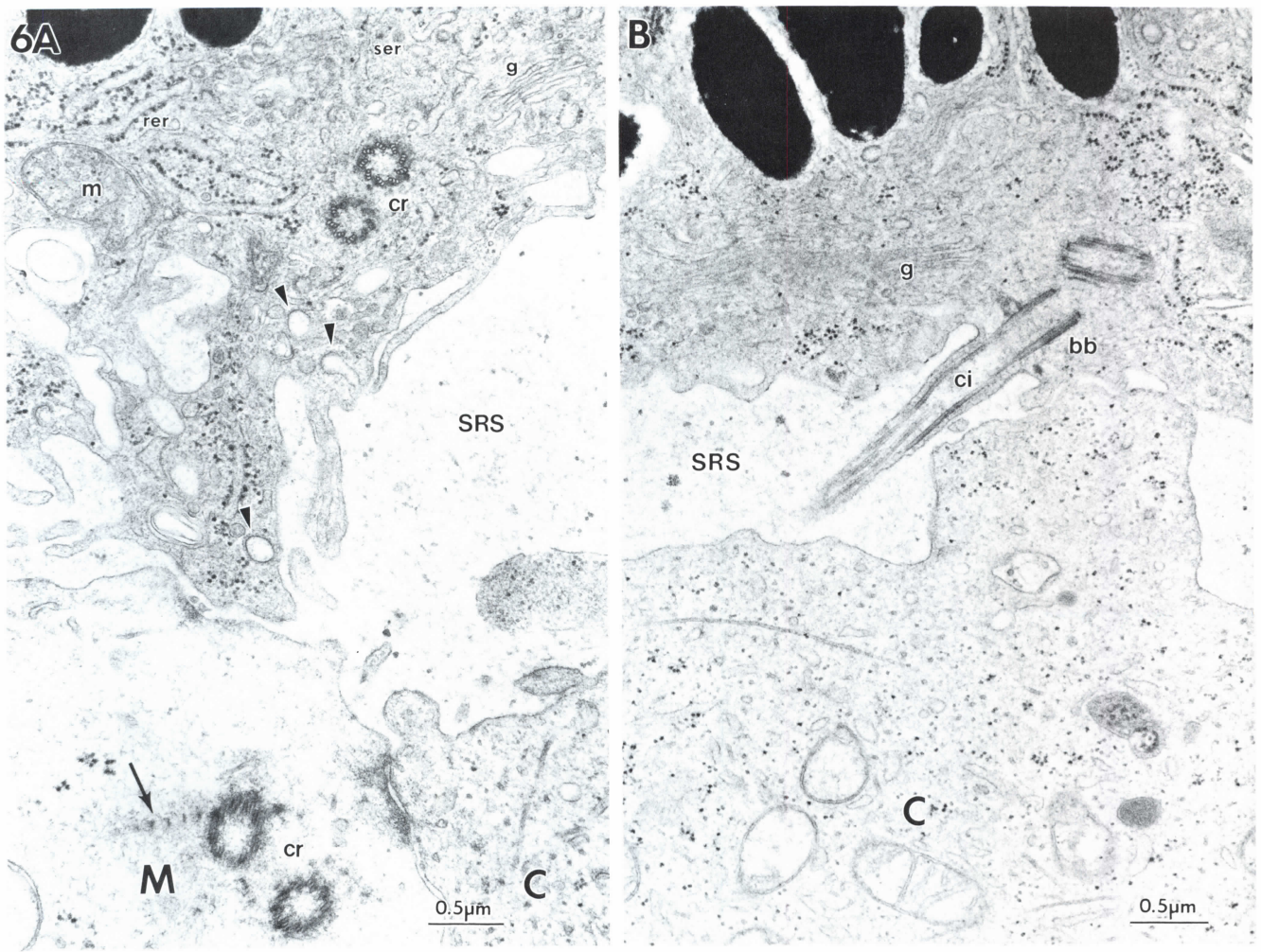

Fig. 6. A: A pair of parallel centrioles (cr) lies in the apical RPE cytoplasm of the 61-mm specimen. The subjacent apical RPE ridge gives rise to an array of processes, some containing coated pits (arrowheads). Two centrioles also occur in the apposing Müller cell cytoplasm (M). One has a ciliary rootlet associated with it (arrow). C: cone precursor; g: Golgi body; m: mitochondrion; rer: rough endoplasmic reticulum; ser: smooth endoplasmic reticulum; SRS: subretinal space. Scale bar = 0.5 μm. B: A cilium (ci) projects into the SRS from a shallow indentation of the RPE apical surface opposing an apical outgrowth of a cone precursor (C). bb: basal body; g: Golgi body. Scale bar = 0.5 μm.

of smooth endoplasmic reticulum (SER), randomly oriented microtubules, and various vacuoles occur regularly. Multivesicular bodies are encountered less frequently (Fig. 7). Pinocytotic vesicles and coated pits can be found on all cell surfaces including that of the apical outgrowths (Fig. 8). The least common organelles seen are bundles of 9–10 nm wavy filaments found in the myoid and basal cone cytoplasm.

The OLM consists of *zonulae adhaerentes* (Figs. 4, 5A, 5B, and 6A) that join cones to each other as well as to the Müller cell processes (Figs. 3, 7, and 8).

The lateral cone cytoplasm

The cytoplasm lateral to the cone cell nucleus contains few organelles except for polysomes and microtubules running parallel to the cell's long axis (Figs. 3, 7, and 8). Occasional mitochondria and cisternae of RER or SER lie within this region especially at its upper and lower margins.

The baso-lateral apposition of one cone to another (Figs. 3 and 7) is distinctive for extensive, flat sheets of endoplasmic reticulum (subsurface cisternae or SSCs) in both cells. SSCs are largely agranular, but have localized regions that may bear ribosomes on their cytoplasmic aspect (Figs. 10A–10D). They appear to be continuous with RER cisternae. At regions of cell-to-cell apposition not lined by SSCs, desmosomes may link adjacent cones (Fig. 10A). Unusually located synaptic ribbons and associated vesicles (Figs. 9E and 10B) are sometimes seen at the apical end of these appositions, often adjacent to coated pits (Fig. 10B), or opposed to "postsynaptic" membrane specializations on the apposing cone (Fig. 10B).

The basal cone cytoplasm

The basal cone cytoplasm comprises the precursor of the cone axon and pedicle. At this stage no axonal constriction is apparent and the nucleus often sits immediately above developing synaptic invaginations (Figs. 3, 7, 11, and 13A). The basal cytoplasm contains large numbers of polysomes. Microtubules, mitochondria, RER, SER, lysosomes, and vacuoles mentioned above are present in smaller numbers than in the apical cyto-

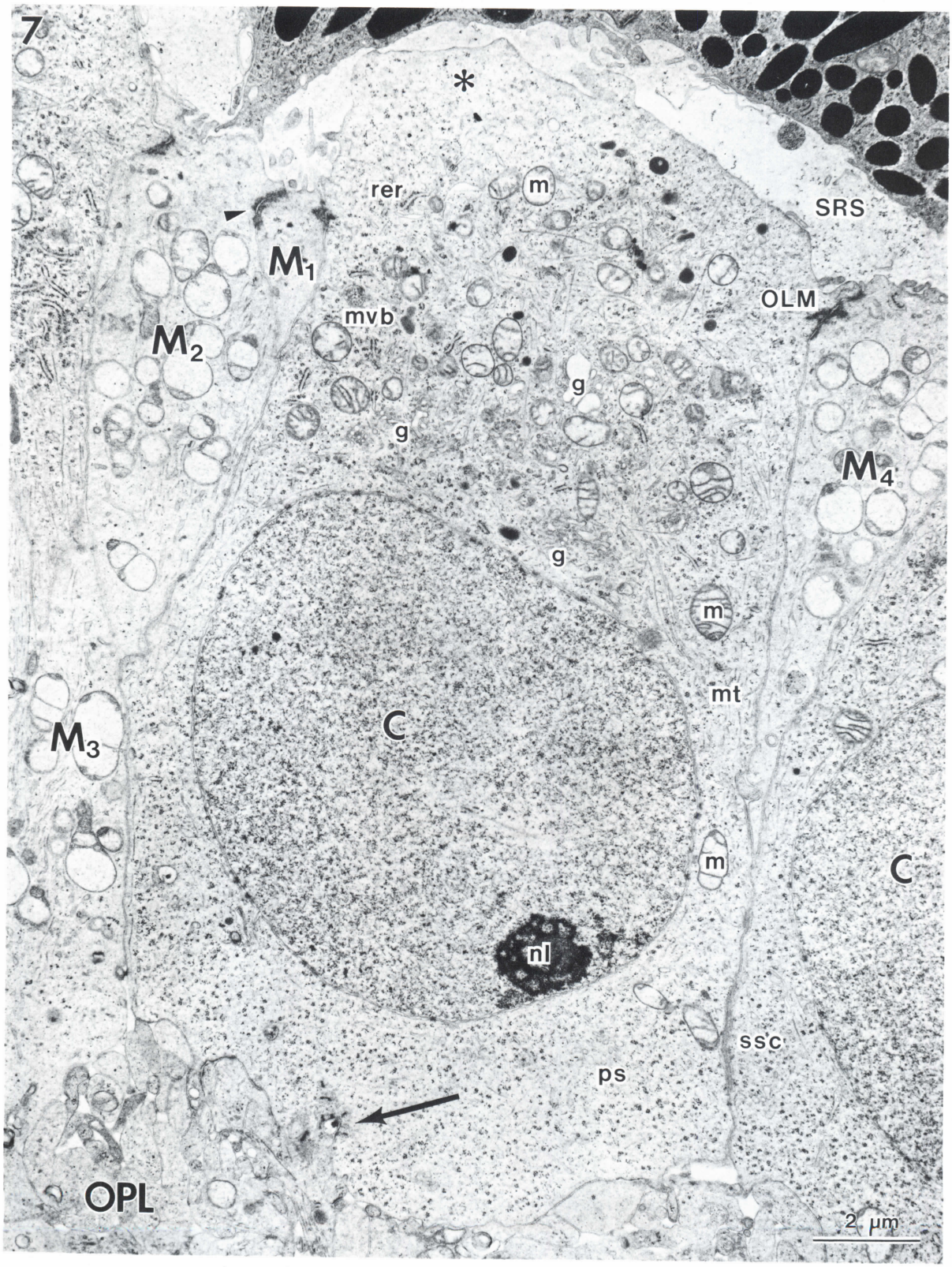

Fig. 7. A cone precursor (C) at 61 mm has the rectangular profile typical for these cells at the posterior pole. Its spherical nucleus is displaced slightly toward the outer plexiform layer (OPL). One of its nucleoli (nl) is visible. Apical cytoplasm houses a rich variety and number of organelles, except in the apical outgrowth (*) bulging beyond the outer limiting membrane (OLM) into the subretinal space (SRS). Basally, the apposition of two cone precursors is lined by subsurface cisterns (ssc). One cone precursor makes synaptic contact (arrow) with processes of second-order neurons. Four different Müller cell processes (M) are labeled. Note that Müller cells also are joined to one another at the OLM (arrowhead). g: Golgi body; m: mitochondrion; mt: microtubules; mvb: multivesicular body; ps: polysomes; and rer: rough endoplasmic reticulum. Scale bar = 2 μm.

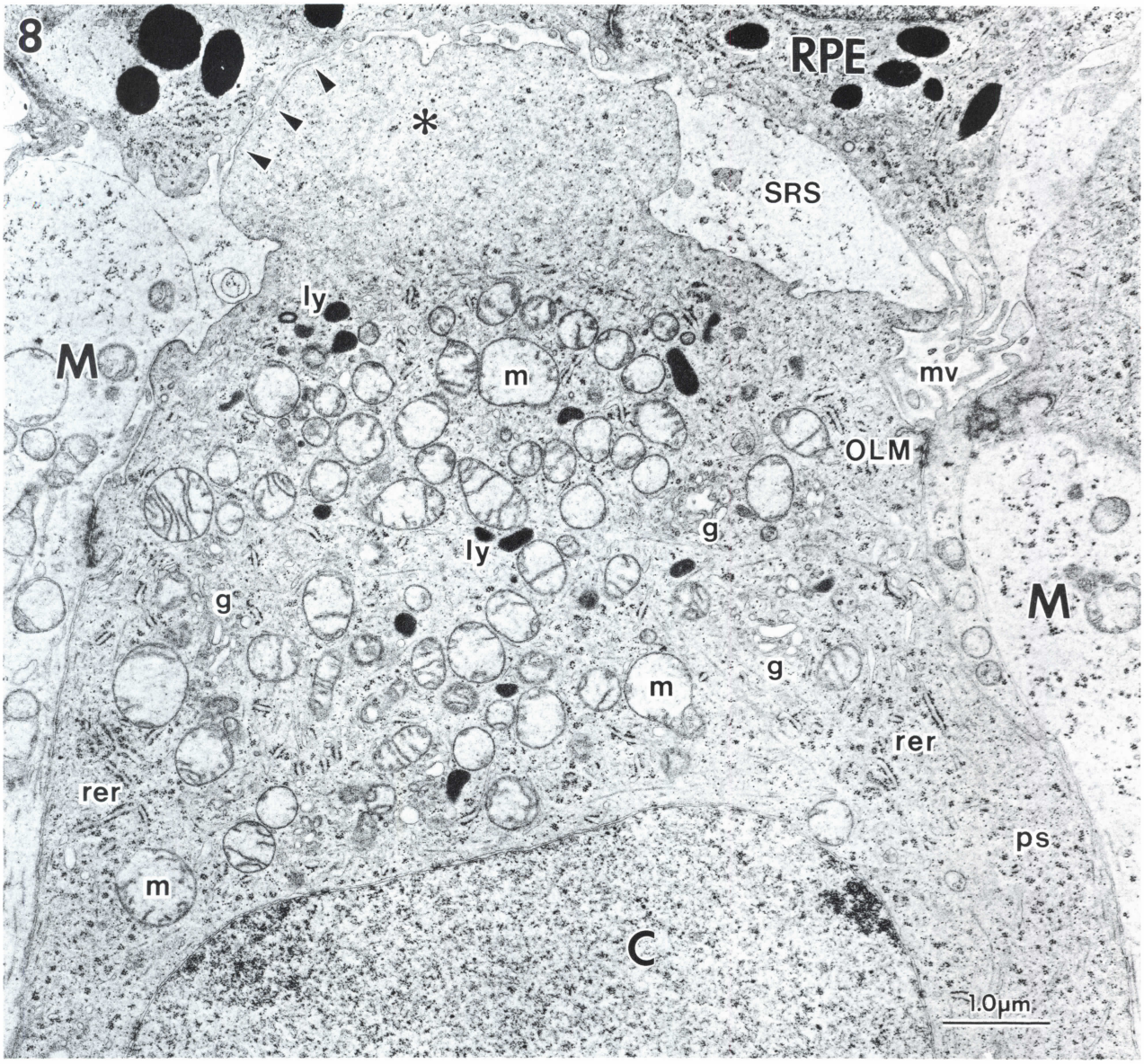

Fig. 8. Apical cone cytoplasm (C) in the 61-mm specimen contains mitochondria (m), lysosomes (ly), polysomes (ps), Golgi bodies (g), rough endoplasmic reticulum (RER), and many randomly arrayed microtubules. The apical outgrowth (*) projecting into the subretinal space (SRS) towards the retinal pigment epithelium (RPE) contains only a fine-grained cytoplasmic matrix. Although the two layers are directly apposed (arrowheads), no junctions link them. Microvilli (mv) projecting from the RPE ridges intermingle with microvilli from Müller cells (M). OLM: outer limiting membrane. Scale bar = 1 μm.

plasm (Figs. 3, 7, 11, and 13A). The lysosomes found here are often elongated in comparison with those of the apical cytoplasm. Synaptic vesicles with a diameter of 45–50 nm are numerous only in the vicinity of the synaptic ribbons.

Synaptic ribbons are usually adjacent to the cone's basal plasma membrane and oppose processes from the differentiating OPL. Although some ribbons appear independent of a synaptic invagination in single sections (Figs. 12A and 12C), other regions that were studied by serial sections revealed that invaginations of the basal cone cytoplasm generally lie nearby. These ribbons vary widely in length and in the number per array (Figs. 12A–12G and 13A) with as many as eight lining a single synaptic invagination (Fig. 12F). Since such arrays were not always serially reconstructed, we cannot exclude the possibility that some ribbon profiles may be segments of a single ribbon. It was our impression, however, that compared to mature ribbons of adult cones, these are shorter and thicker. Arciform densities are not always distinct this early in synaptic development, and while some of the developing ribbons have the pentilaminar substructure known for mature ribbons (Cohen, 1963) (Fig. 12D), many do not. From their earliest recognizable form, as small, electron dense patches lying near the basal plasma membrane (Figs. 12A, 12D, and 12F), they are associated with the light-cored vesicles.

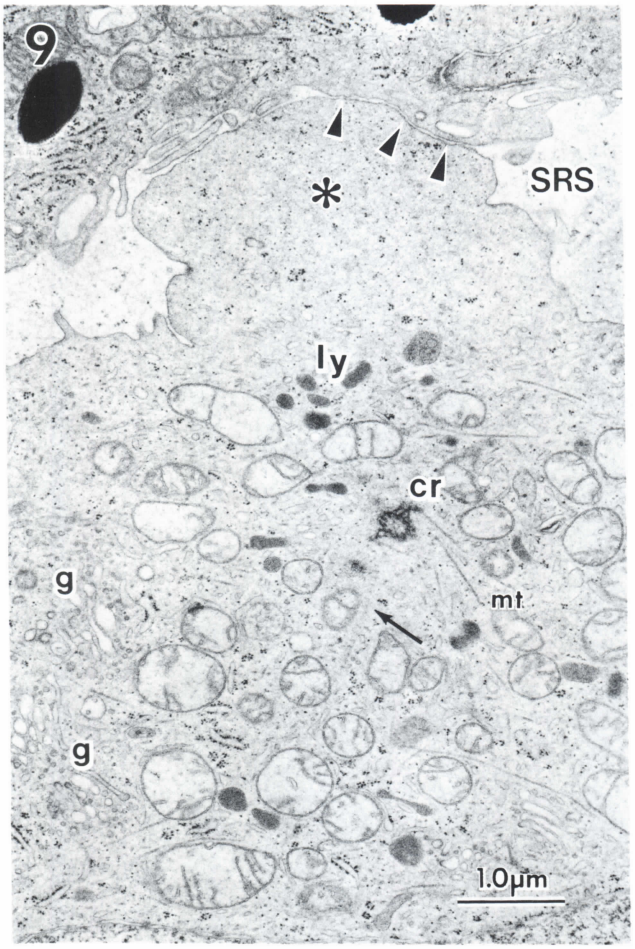

Fig. 9. At 61 mm, a small apical outgrowth (*) of a posterior cone precursor projects into the subretinal space (SRS) towards the retinal pigment epithelium (RPE). Although the two cells are directly apposed (arrowheads), no junctions link them. A centriole (cr) lies in the cone's apical cytoplasm but benearth the outgrowth. Associated microtubules (mt) and a striated rootlet (arrow) lie nearby. The edge of the cell's nucleus is visible at the bottom. g: Golgi body; and ly: lysosome. Scale bar = 1 μm.

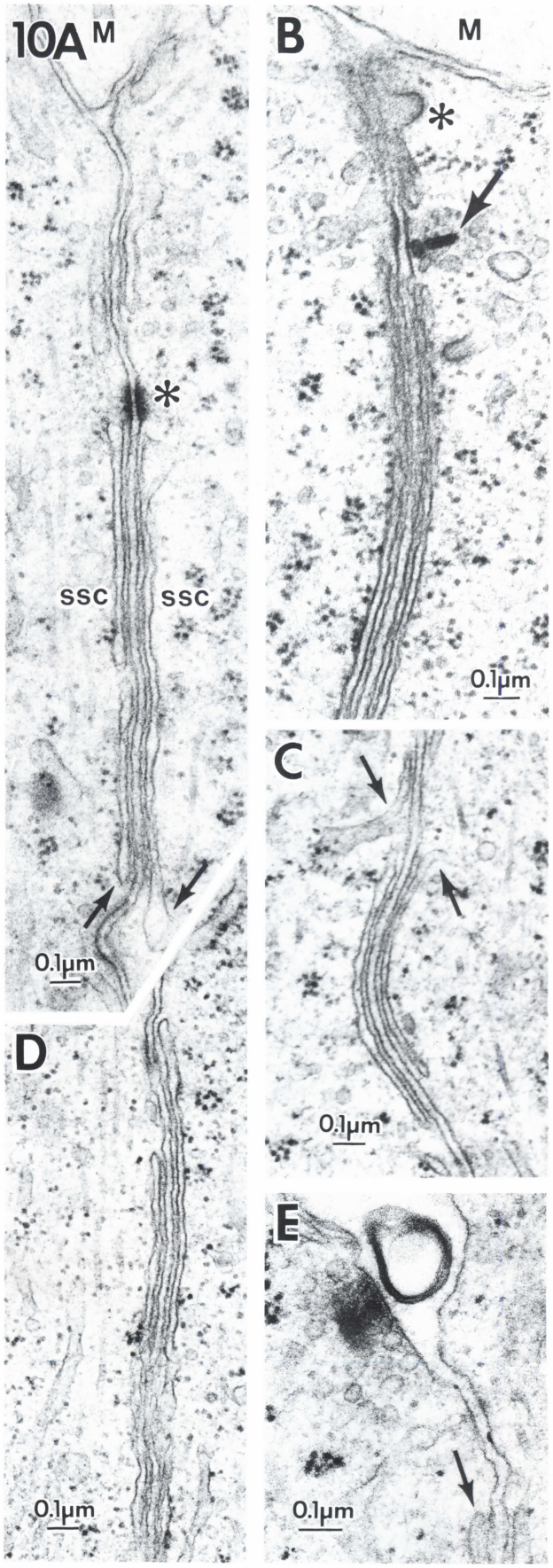

Fig. 10. Specialized structures seen at the lateral apposition of cone precursors in the posterior outer retina of the 61-mm human fetus. A: A desmosome-like junction (*) interrupts the lining of the lateral apposition of two cones by subsurface cisterns (SSCs). The proximal ends of the SSCs dilate (arrows). M: Müller cell cytoplasm. B: The apical end of an apposition features a coated pit (*) distal to an ectopic synaptic ribbon (arrow) surrounded by light-cored vesicles. The opposing cone plasma membrane is electron dense. Note the ribosomes on the cytoplasmic face of one SSC. M: Müller cell process. C: SSCs line the apposition of two cones with cisternae coursing into the cytoplasm (arrows). D: SSCs lining a lateral apposition. Note the cisternae of cytoplasmic rough endoplasmic reticulum (RER) parallel to this apposition. E: Another ectopic synaptic ribbon, here seen *en face*, lies at the apical end of a lateral opposition. The distal tip of an SSC is indicated at the arrow. Scale bar = 0.1 μm for A–E.

Fig. 11. Basal cytoplasm of a posterior cone precursor (C) and the outer plexiform layer (OPL) at 61 mm. Synaptic ribbons (sr) and associated vesicles occur at two invaginations, the one to the right is made by two OPL processes of similar ultrastructure. Two adjacent coated pits are indicated at the arrowhead. The OPL is thin and loosely organized. A horizontal cell perikaryon (HC) sends a process (*) up into the OPL. m: mitochondrion; ps: polysomes; and rer: rough endoplasmic reticulum. Scale bar = 1 μm.

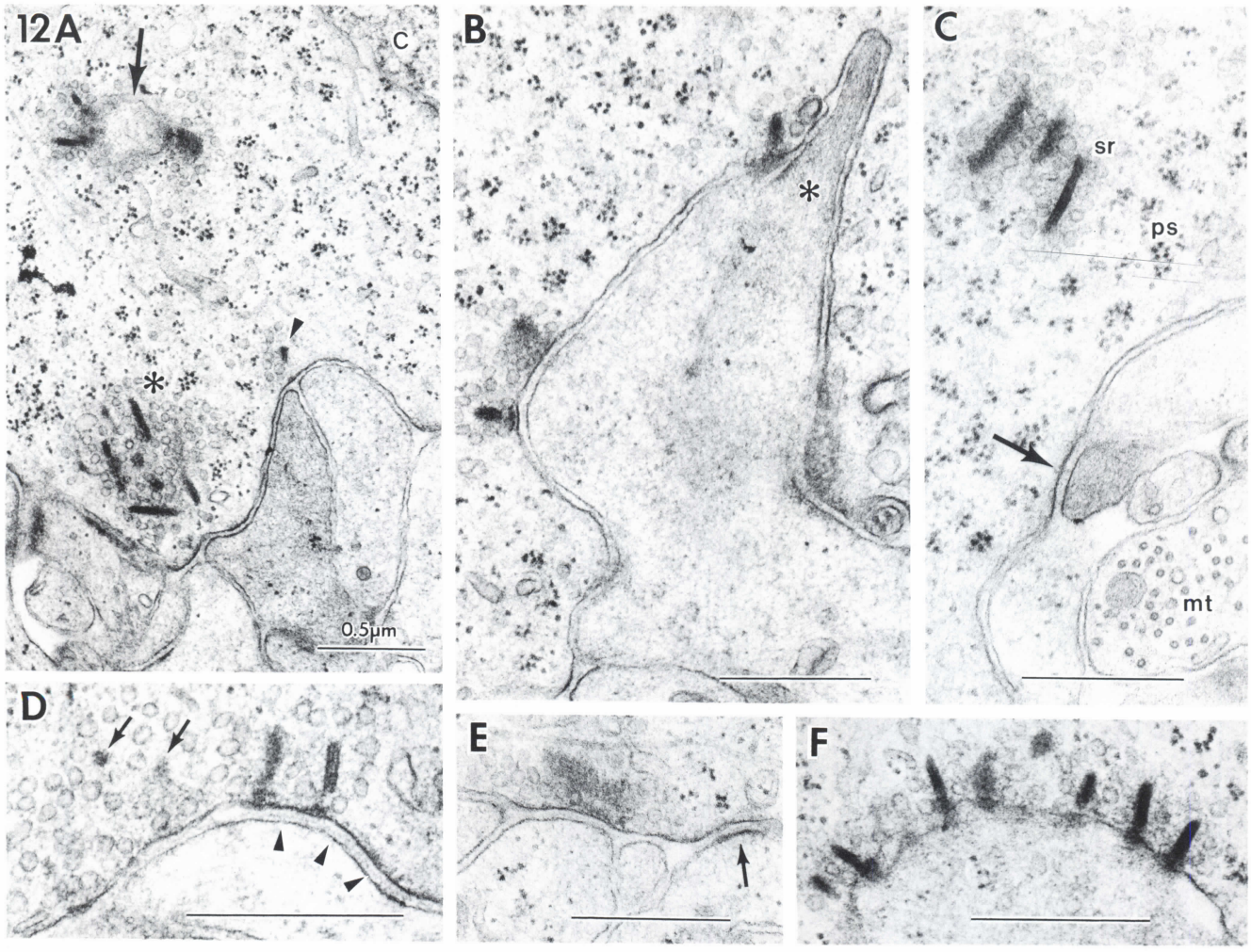

Fig. 12. Synaptic arrays in the basal cytoplasm of developing cones at the posterior pole of a 61 mm human fetus. A: Three synaptic ribbons (arrow) oppose the distal tip of a deeply invaginating process, while a cluster of seven synaptic ribbons, including two punctate ones (*), apparently lie free in the presynaptic cytoplasm. At a third location (arrowhead), the tip of a single ribbon faces two postsynaptic processes of differing electron density. Note that synaptic vesicles are located only around the ribbons. B: An outer plexiform layer (OPL) process deeply invaginates the basal cone cytoplasm. Distally the process contains microfilaments (*). Three synaptic ribbons oppose the process in this plane of section. C: Three synaptic ribbons (sr) surrounded by vesicles lie in the cytoplasm away from the plasma membrane. Nearby a presumed basal contact (arrow) is made by a small, electron-dense process. Note the many cross sections of microtubules (mt) in a subjacent OPL process. ps: polysomes. D: Two synaptic ribbons oppose a single postsynaptic process across a cleft in which electron-dense material forms a line midway between the apposed membranes (arrowheads). Two other ribbons (arrows) appear as small, electron-dense patches. E: A synaptic ribbon, seen *en face*, extends 0.3 μm along the cone plasma membrane. Nearby an OPL process makes a basal contact at an indenting apposition of electron-dense membranes (arrow). F: Eight ribbons line the shallow invagination of basal cone cytoplasm by a single postsynaptic process. Scale bar = 0.5 μm for A–F.

FACING PAGE

Fig. 13. The outer posterior retina at 61 mm. A: The base of a cone precursor (C) lies across a thin outer plexiform layer from a horizontal cell perikaryon (HC). Columns of Müller cell cytoplasm (M) lie at either side, both of which send rudimentary horizontal fibers (*) into the OPL neuropil. Apical HC cytoplasm contains various organelles including autophagic vacuoles (arrowheads). mt: microtubules; ser: smooth endoplasmic reticulum; and sr: synaptic ribbons. Scale bar = 1 μm. B: Low-power montage of cells bordering the thin OPL neuropil. Cone precursors (C) receive basal contact from horizontal (HC) and bipolar cell (B) processes. Two HCs are outlined permitting the visualization of their stout, organelle-rich dendritic trunks (*) which course laterally to contact cones distally (arrowheads). The apical cytoplasm of two bipolar cells is more electron lucent than that of the HCs. Both contain centrioles (cr). Scale bar = 5 μm.

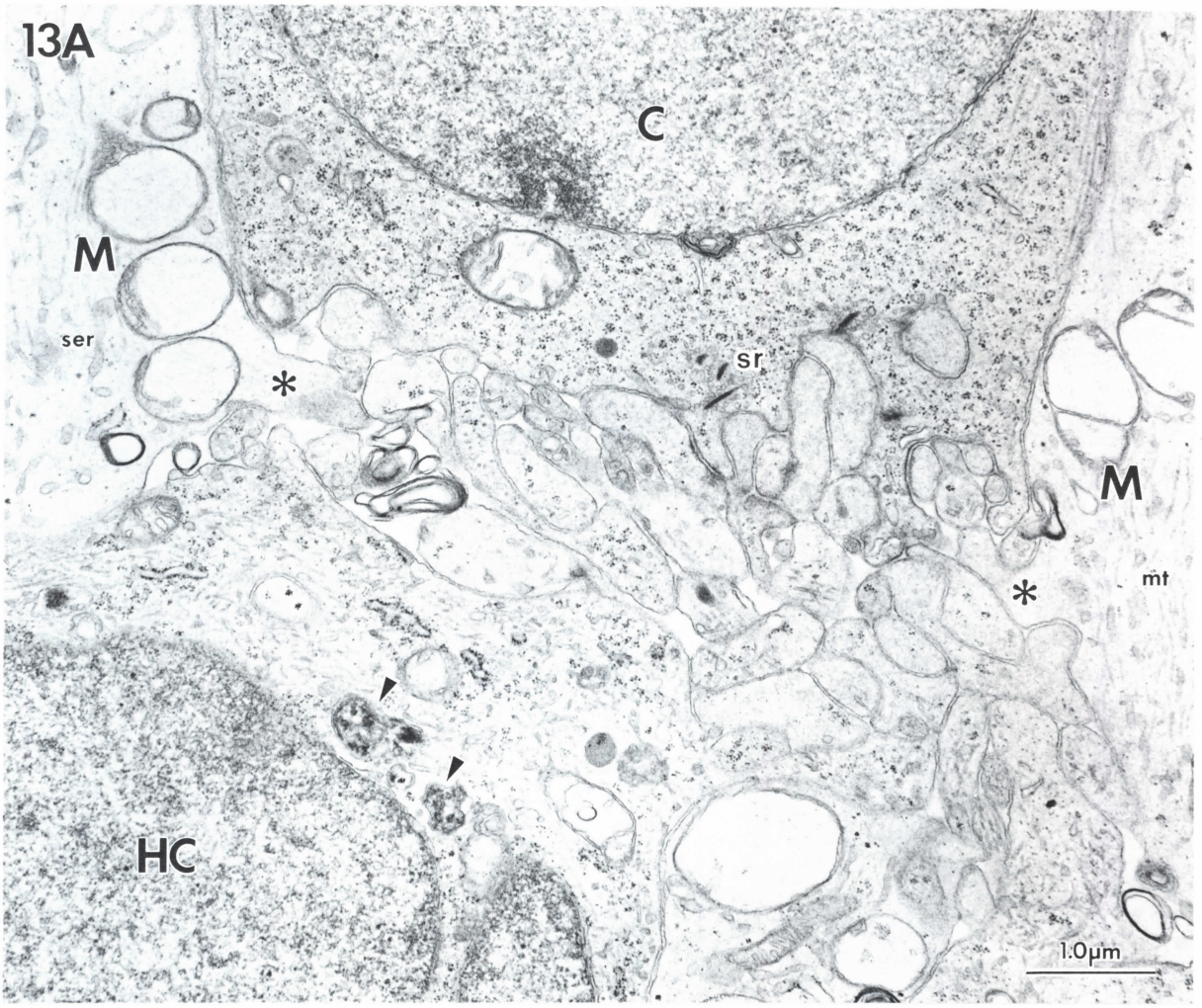
13A
C
M
ser
sr
M
mt
HC
1.0μm

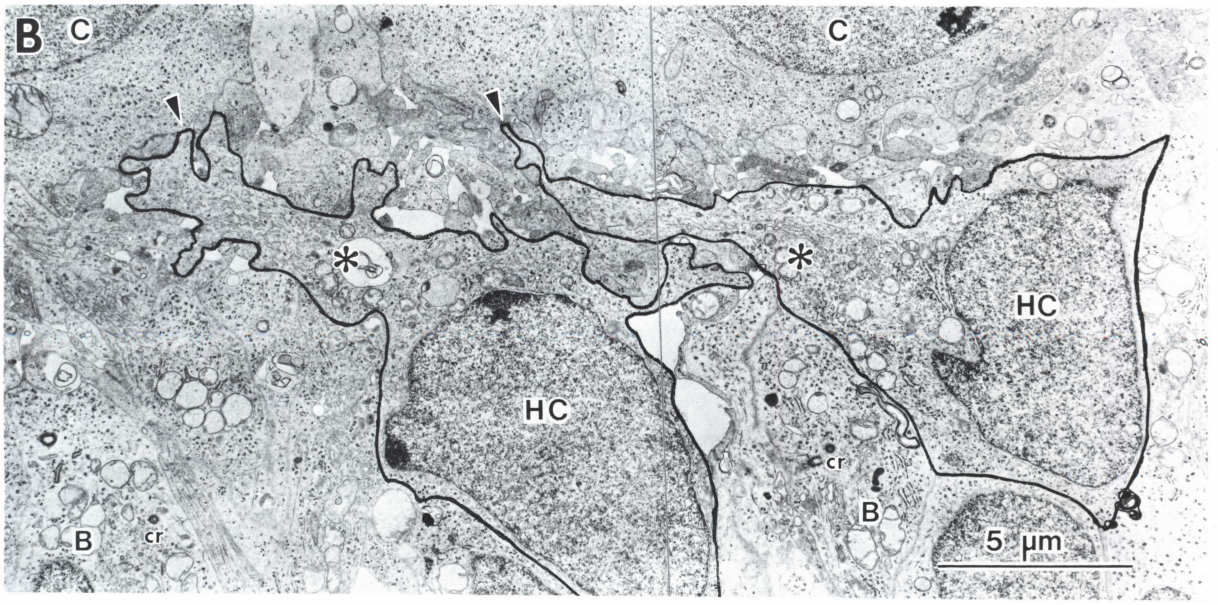
B
C
C
HC
HC
cr
B
B
cr
5 μm

The invaginations of the basal cone cytoplasm by the postsynaptic processes vary in depth, but usually at this stage are quite shallow (Figs. 7, 11, and 13A). Since these processes lack the microtubules characteristic of bipolar cell dendrites (Figs. 11, 12A, 12B, and 13A), our impression is that they arise from differentiating horizontal cells (see below).

Basal contacts from processes of the OPL neuropil assume a variety of configurations. At ribbon synapses, both the presynaptic and postsynaptic membranes are electron dense and the synaptic cleft is sometimes, but not always, widened. It often contains electron dense material, usually as a line midway between the opposed membranes (Figs. 11, 12B, 12D, and 12E). At non-ribbon associated basal contacts by presumed bipolar dendrites, both membranes and the diffuse intracleft material are more electron dense than at surrounding regions of apposition (Figs. 12C and 12E). In yet another type of apposition, only the cone precursor's basal membrane bears extensive densification (Fig. 12D).

Müller cell processes

The outer cytoplasmic processes of Müller cells are easily recognizable at 61 mm, but not at 55 mm. They border the SRS and participate in the *zonulae adhaerentes* comprising the OLM (Figs. 3, 4, 5A, 5B, 6A, 7 and 8). Compared with the adjoining cone precursors, Müller-cell outer processes are much more electron lucent and contain far fewer organelles. At 61 mm, Müller cell nuclei lie in the thick inner nuclear layer (INL). Wide cytoplasmic columns extend from them and pass up through the OPL and cone monolayer to broaden apically. Mitochondria are clustered in this region of the cell (Figs. 3 and 7). Paired centrioles with their associated striated rootlets are occasionally seen apically in these processes (Fig. 6A). From the apical surface of almost every process project relatively straight, always unbranched, microfilament-containing microvilli (Fig. 5A). The sub-apical Müller cell cytoplasm contains scattered mitochondria and polysomes as well as axially oriented microtubules and Golgi bodies (Figs. 3, 7, 8, and 13A). More noticeable are the cisternae of smooth endoplasmic reticulum that contain a uniformly electron-dense, fine-grained matrix (Fig. 13A). No glycogen deposits are evident. At the level of the developing OPL, Müller-cell outer processes give rise to slender lateral processes, or "horizontal fibers," that project between processes of the OPL neuropil (Fig. 13A). At 61 mm these processes are very rudimentary.

The OPL and second-order neurons

At 61 mm, the emerging OPL occurs only at the posterior pole, although it extends beyond the cone monolayer. Since the developing photoreceptors lack axons, the OPL sublamina *a* is absent. At a period prior to rod morphogenesis, sublamina *b* contains only differentiating cone pedicles. The developing neuropil, or OPL sublamina *c*, is thin, only 1.5–3 μm in width at its most posterior position (Figs. 3, 7, 11, 13A, and 13B), narrowing with increasing eccentricity. Even posteriorally this layer seems discontinuous in single thin sections (Fig. 13A) due to the thick, outer Müller-cell processes that cross this developing layer to adjoin the OLM distally. In fact, the developing photoreceptors at the posterior pole of the 61 mm fetal retina are never directly apposed to neurons of the inner nuclear layer (INL). The processes that comprise the OPL neuropil arise from second-order neurons of the developing INL. Compared to the adult OPL, the processes are loosely packed, often with large lacunae of extracellular space between them (Figs. 3, 11, 13A and 13B). This is especially true in less-differentiated (more peripheral) regions of the posterior retina where the processes are blunt and less-branched, and the proximity of cone pedicle to bipolar or horizontal cell perikarya is increasingly direct.

OPL processes vary both in their organelle content and their size. As a rule, processes in the outer portion of the neuropil are narrow and have fewer organelles and less cytoskeleton than those along its inner border (Figs. 11 and 13A). Ribosomes, vesicles, and microtubules are the most common organelles encountered in the former (Figs. 11, 12A–12F, and 13A), while mitochondria, lysosomes, endoplasmic reticulum, and even Golgi bodies occur in the latter (Figs. 11, 13A, and 13B). OPL processes at this age often have a "glycocalycal" coat that is most evident in regions where they lie adjacent to lacunae of extracellular space (Fig. 11). Conventional synapses and junctions of varying morphologies occur between processes and between processes and the somata of second-order neurons. These have been described previously (Linberg & Fisher, 1986).

Two types of cell lie at the outer edge of the INL and contribute processes to the developing OPL. The outermost type is larger and its lobed nucleus is rounded and often flattened horizontally (Figs. 11, 13A and 13B). Its large dendritic trunks spread laterally and diagonally through the OPL neuropil to end against developing cone pedicles with dendrites lacking organelles (Fig. 13B). These have a morphology typical of horizontal cells (HCs). The other cell type has a more elongate nucleus, a more electron-lucent cytoplasm, and it's apically situated dendritic trunks contain many microtubules (Fig. 13B). This morphology is more typical of bipolar cells. Both cell types have an expanded apical cytoplasm rich in organelles (Figs. 3, 11, 13A, and 13B). Both also contain paired centrioles (Fig. 13B). HCs contain autophagic vacuoles as well (Fig. 13A). With increasing distance from the posterior pole, these differentiating second-order neurons are more and more similar to the subjacent neuroblasts, and the OPL less and less discernable.

The peripheral outer retina

In the mid-periphery, the SRS separating retinal cells from the RPE monolayer is greatly reduced (Fig. 14A). The RPE apical surface is relatively featureless. Retinal cells contain groupings of mitochondria, but few other indications of differentiation. Mitotic figures still are found at these eccentricities. Relatively simple adhesion-type junctions link the cells of the two layers along this interface (Fig. 14A). Such junctions are lacking at both the posterior pole and far periphery of this same specimen. In the far periphery, the outer retina is even less-differentiated and in many respects resembles the outer retina of the 55-mm specimen (Fig. 14B). Mitotic figures are evident as are cilia projecting from the neural retinal cells into the SRS. There is no recognizable OPL, and evidence of synaptic ribbons, vesicles, or invaginations was not found.

Discussion

The pure-cone region of the developing human fetal eye described here is localized to an area in the posterior retina that

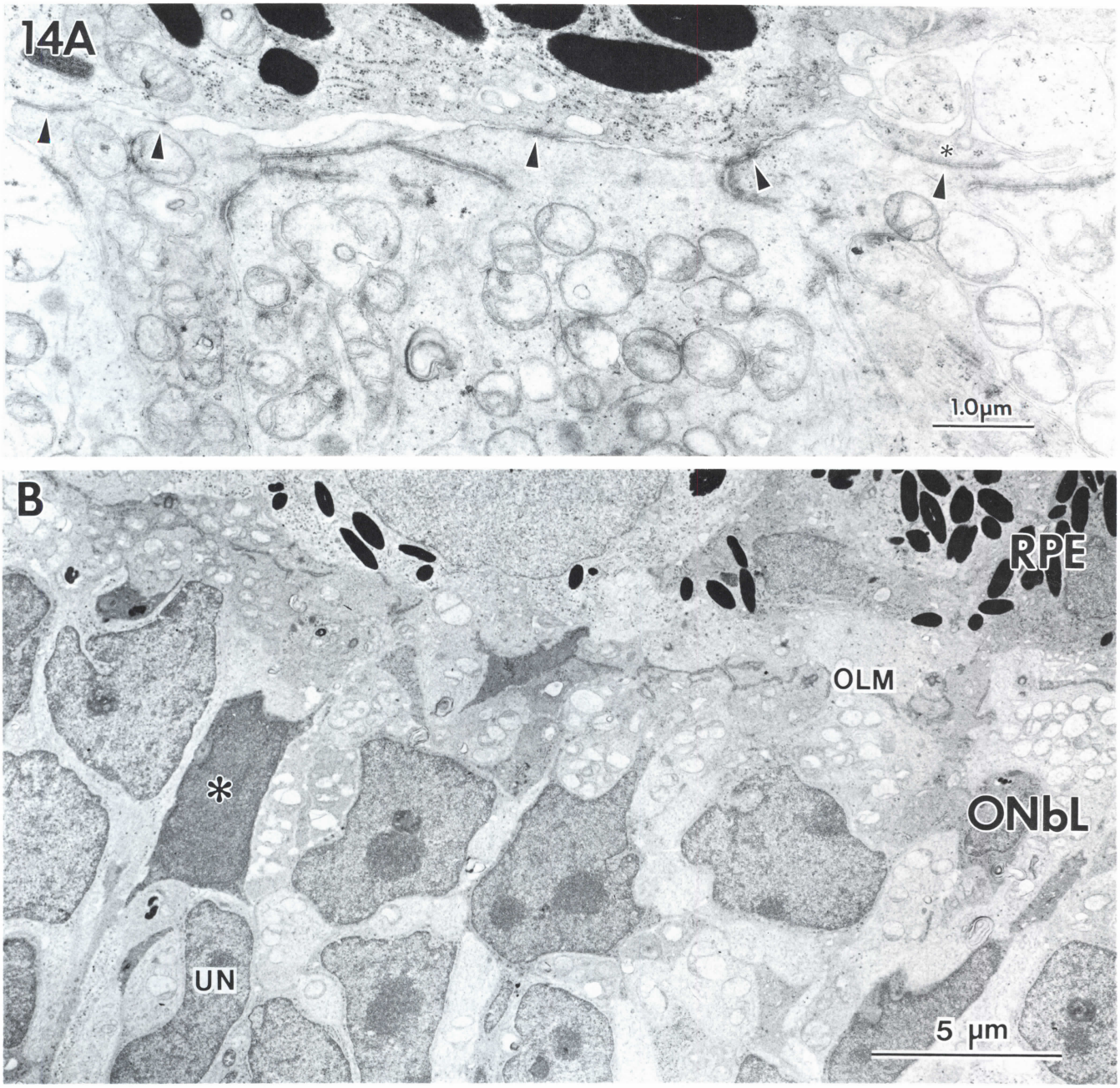

Fig. 14. Peripheral regions of the 61 mm human fetal retina. A: In the mid-periphery, the volume of the subretinal space (SRS) is dramatically reduced as are the apical processes of the photoreceptor precursors and the retinal pigment epithelium (RPE). As direct apposition of the two layers becomes the norm, the number of cell junctions across the SRS increases. These junctions (arrowheads) are small and appear less complex than the *zonulae adhaerentes* comprising the outer limiting membrane (OLM). An RPE apical process (*) forms a junction with the neural retina and then partially wraps a process in a pocket of the SRS. Scale bar = 1 μm. B: At the far periphery, the appearance of the outer retina is primitive. Undifferentiated neuroblasts (UN) underlie primitive photoreceptors that have irregularly shaped nuclei lying in uncompartmentalized cytoplasm. Electron-dense cells, most likely necrotic (*), lie among these photoreceptor precursors. The SRS is very narrow. No outer plexiform layer is present. Müller cell processes are not distinguishable. ONbL: outer neuroblast layer. Scale bar = 5 μm.

eventually forms the fovea (Barber, 1955; Hervouët, 1958; Duke-Elder & Cook, 1963; Mann, 1969; Hendrickson & Youdelis, 1984). At birth, the fovea is immature relative to surrounding regions of the retina, yet the fovea itself is the first part of this tissue to differentiate. In fact, the development of the macula is precocious up to the end of the third month of gestation, after which its rate of maturation lags behind surrounding regions until the eighth month when the pace of its development again quickens (Hervouët, 1958; Duke-Elder & Cook, 1963; Mann, 1969; Hendrickson & Youdelis, 1984). Al-

though the third month is often cited as a critical developmental period for the posterior retina, almost no ultrastructural data exist for the human fetal retina at this age. By the fourth gestational month, cone precursors, a developing OPL, and a differentiating inner nuclear layer have already been described posteriorally (Hollenberg & Spira, 1972, 1973; Spira & Hollenberg, 1973). Indeed, in this study we were able to establish, with two well-preserved specimens, that these features are clearly evident by the eleventh week. We recognize that our conclusions are based on the sample of only two retinas, in part because we chose not to study retinas of comparable ages if their fixation quality was poor. As well, we chose only retinas from apparently normal fetuses from donors whose prior medical history gave no indication of pathological conditions that might have affected normal fetal development. In estimating fetal age, we relied primarily on crown-rump length, a measurement made just prior to the enucleations. In our interpretation of this data, we must acknowledge the caveat of O'Rahilly (1975) that the length of a fetus is not enough to accurately determine a given stage of development. We understand this to indicate that the size and stage of retinal development could vary considerably between fetuses of the same CR length. In the case of the 55- and 61-mm fetuses, the diameter of the eyes varied by 1 mm, being 3.5 and 4.5 mm, respectively, giving further credence to the conclusion that the 61-mm specimen is slightly older than the 55-mm specimen. Even if our developmental staging is not absolute, our data still indicate that significant and rapid changes are occurring in the development of the outer retina at around $2\frac{1}{2}$ months.

Our data showing a monolayer of developing cones as well as a narrow OPL in the posterior pole at 61 mm confirm the earlier light-microscopic observations of Barber (1955) and Hervouët (1958). Electron microscopy revealed that this lineup of cones was accompanied by a burst of differentiation involving every cell type in or bordering the monolayer. This series of transformations was restricted to this small posterior region and all quickly disappeared in sections taken at increasing eccentricities.

It is well-known that in the mammalian retina, cone precursors differentiate many weeks before rods (Hollenberg & Spira, 1972, 1973; Smelser et al., 1974; Hendrickson & Kupfer, 1976). Until the end of the second month of gestation, the precursors of human photoreceptor cells cannot be morphologically distinguished from the undifferentiated cells comprising the outer neuroblast layer (Hervouët, 1958; Mann, 1969; Rhodes, 1979).

Among the widely accepted criteria for recognizing cells undergoing differentiation in the retina are: (1) the cell nucleus changes from darkly-staining and oval-shaped to lightly-staining and more circular in profile; (2) the cell rounds up so that the nucleus of a differentiating cell appears to lie in a greatly expanded cytoplasm; and (3) the cytoplasm stains lightly. The earliest that Mann (1969) could identify photoreceptor precursors was at 48 mm where they lay in the outermost layer of the retina and had nuclei that were partially rounded, or "kidney-shaped." They occur in a retinal region that Mann claims is devoid of mitotic figures from that age on. Rhodes (1979) finds similar cone precursors among the outermost row of posterior neuroblasts at 51 mm, their nuclei being round although indented, staining less intensely than the dark, oval nuclei of undifferentiated neuroblasts beneath. Moreover, the perikaryal cytoplasm of these cells has increased in volume. He reported that this trend continues through the balance of the third month, a period when the fetus grows to 70 mm CR. At 55 mm, we also found some scattered cells at the outer edge of the posterior retina with this morphology. These probable cone precursors, besides having a slightly expanded cytoplasm, show initial signs of the compartmentalization of organelles characteristic of adult photoreceptors. In the younger specimen, however, there was no recognizable OPL, nor precursors of horizontal or bipolar cells, nor outer processes of Müller cells, nor an appreciable SRS. In contrast, the large perikarya of the cone monolayer dominate the posterior pole at 61 mm. A similar monolayer of photoreceptor precursors has also been reported for the developing macaque retina (Smelser et al., 1974; Hendrickson & Kupfer, 1976). The cytoplasm of the cone precursors at 61 mm shows a greater degree of partitioning of cellular organelles than seen at 55 mm.

At 11 fetal weeks there are no outer segments. Organized outer segment discs have not been described before 28 gestational weeks (Yamada & Ishikawa, 1965; Johnson et al., 1985), although Johnson and colleagues (1985) show tubular-like structures in photoreceptor cilia at 22 weeks that they propose as precursors of outer segment discs (see also Nir et al., 1984). Although the developing cone cells in the 11-week posterior retina have basal bodies within their apical cytoplasm, we found that the vast majority of these cells do not have a cilium at this age.

The most apical cone cytoplasm projects past the OLM in what other authors have proposed as the anlage of the inner segment (Smelser et al., 1974; Vogel, 1978; Greiner & Weidman, 1980). These projections have a different composition than the organelle-rich cytoplasm beneath them; their fine-grained cytoplasmic matrix contains few organelles except for occasional vesicles. It appears that the organelles that will populate the adult ellipsoid and myoid develop together in the densely populated cytoplasm above the photoreceptor nucleus and later partition themselves into their respective compartments in a process that must involve a great deal of migration by specific organelles.

Our study confirms that the cone precursors are linked by intercellular junctions comprising the differentiating OLM, and that they retain these junctions during cell division (Hollenberg & Spira, 1973). By 61 mm, these cells also are joined to developing Müller cells in a typical OLM. Just when processes of Müller cells reach the OLM has been the subject of controversy. Vrabec (1983) concludes that Müller cells can be identified very early in embryonic life by the Golgi method; he readily identifies Müller-like cells spanning the whole retina at the 23-mm stage. Mann (1969), however, reports Müller cells reaching the OLM much later, at 5 $\frac{1}{2}$ months (170 mm). Recently, Rhodes (1979, 1984) has identified Müller cell processes separating cone precursors at 71 mm. At 61 mm but not at 55 mm, we find similar Müller cell processes separating cone precursors at the level of the OLM. In contrast to the electron-dense processes reported by Rhodes, Müller cell processes at 61 mm are particularly obvious because they are so electron lucent relative to the cones and the undifferentiated cells of the inner retina. Such staining differences may simply reflect different fixation protocols. Nevertheless, it appears that Müller cells and cones undergo important morphological differentiation at about the same time in the region destined to become the adult fovea.

The separation of adjacent cones by Müller cells is incomplete at 61 mm since basally cone precursors are broadly apposed in a configuration specialized by the presence of extensive

SSCs. These structures have been found in a variety of retinal neurons (Fisher & Goldman, 1975), but their function is unknown. We have not observed SSCs in adult human photoreceptors, nor, for that matter, in those fetal cells at 61 mm outside the region of the developing macula. Since Hollenberg and Spira (1972, 1973) found neither SSCs nor any interreceptor apposition in their material, and none at 83 mm particularly, these extensive SSCs, whatever their function, may be limited to a specific developmental phase of the cones, or may be specific to developing macular cones.

The base of these cones bears little morphological resemblance to adult foveal cones with their broad pedicles and long axons making up the fibers of Henle (Polyak, 1941), although by 61 mm several synaptic invaginations, multiple ribbons, and numerous vesicles are already evident. It was our impression that the earliest form of ribbons were small electron-dense patches similar to those described in the mouse (Olney, 1968), rat (Weidman & Kuwabara, 1968), and guinea pig (Spira, 1975), because they were always associated with synaptic vesicles. We did not find any evidence that nascent synaptic ribbons migrate from some distant source (Smelser et al., 1974). Indeed, all ribbons and dense patches were seen near the plasma membrane of the cone precursors. We found no evidence indicating a sequence whereby the elongated lysosomes of the basal cytoplasm give rise to ribbons (Smelser et al., 1974).

Ectopic ribbons were occasionally seen laterally well above the nucleus. They were also always closely associated with vesicles and the cell membrane. Such ectopic synapses must be a transient developmental phenomenon. Because synapse formation is critical to the survival of differentiating neurons elsewhere in the central nervous system (CNS) (see Purves & Lichtman, 1985), perhaps these early, misplaced synapses in some way assure the survival of these cells until adequate connections are formed with horizontal and bipolar cells. We have never seen evidence of cell death along the cone monolayer although it is common elsewhere in the retina. Indeed, cell death has never been reported as a major factor in the development of the fovea (Hervouët, 1958; Mann, 1969; Rhodes, 1979; Youdelis & Hendrickson, 1986).

The most mature cone synapses were confined to the most posterior part of the retina of the 61-mm specimen. Even here one or two postsynaptic processes were the norm. The synaptic triads characteristic of primate cone synapses (Dowling & Boycott, 1966) must form later. There are, as in the adult human retina, multiple basal invaginations per cone even at this early period. In contrast to adult cone synapses where one or two ribbons associate with each invagination (Missotten, 1965), multiple synaptic ribbons often occur at each of these invaginations. Basal contacts, similar to those made in the adult human by flat bipolars, are also seen, although we cannot rule out the possibility that these represent the earliest stage in the formation of an additional invagination (see below).

A number of investigators have suggested that cone synapses progress from single appositional contacts to invagination by one or two processes, and finally the addition of the third element to form the triad (Blanks et al., 1974; McArdle et al., 1977; Vogel, 1978). Similar stages can be identified in the 61-mm specimen by moving from posterior to more peripheral regions. More peripherally, OPL processes and presynaptic structures both disappear leaving direct apposition of cone precursors to the perikarya of differentiating second-order neurons.

The RPE and subretinal space

In the adult retina, RPE cells show compartmentalization of organelles with melanin residing near the apical border and within the larger apical processes, and mitochondria tending to aggregate around the periphery of the cells (Zinn & Benjamin–Henkind, 1979). In these two specimens, there is no obvious compartmentalization of these organelles. Adult RPE cells also show considerable infolding of their basal membrane (Zinn & Benjamin–Henkind, 1979). This process appears to be just beginning at the 11-week stage of development.

The branched processes on the apical RPE surface at 61 mm are probably the first manifestation of the complex apical processes typical of the adult RPE. As in the developing cat, these begin as fairly large ridges of cytoplasm sparsely located on the cell surface from which thinner sheets or villous processes arise (Pfeffer & Fisher, 1981). As soon as the finest sheet-like and villous processes appear, they contain a core of microfilaments characteristic of the adult processes (Anderson & Fisher, 1979; Fisher & Steinberg, 1982; Murray & Dubin, 1975; Burnside & Laties, 1976). The RPE, therefore, appears to initiate differentiation of its apical surface several weeks before developing photoreceptor cells extend the cilia that give rise to outer segments.

There have been few published observations on the development of the subretinal space (SRS) and its contents in the human retina. According to our results, the space forming the SRS first exists between two relatively undifferentiated surfaces and as development proceeds, cells from the neural retina and RPE begin to contribute processes to it at about the same time. Johnson et al. (1985) cite Yamada and Ishikawa (1965) as showing the space at 27 fetal weeks, while data in Hollenberg and Spira (1973) showed that the SRS forms at 18 weeks. In this study, we find clear evidence for its formation between the tenth and eleventh gestational week. Thus, the space begins to form as the junctional complexes linking the retina and RPE are disappearing (Fisher & Linberg, 1975; Hollenberg & Spira, 1973; Townes–Anderson & Raviola, 1981); indeed in the mid-periphery of the 61-mm specimen, we still find evidence of adhering junctions between these cells. These junctions probably serve an adhesive function necessary to keep the cells in close proximity during early development, and as the layers mature, the physiological mechanisms of retinal adhesion found in the adult retina take over this function (see Steinberg, 1986). Our data suggest that these mechanisms must be in place as early as 10–11 fetal weeks because, with the exception of the mid-periphery, the two layers remain closely apposed in the absence of adhering junctions.

The results of this study show that in the 55-mm specimen the SRS is just beginning to increase in volume as isolated areas of expanded extracellular space interrupt the close apposition of RPE and neural retina. In the posterior pole of the 61-mm specimen, separation of the layers has become the norm; cone cells, RPE cells, and Müller cells are all beginning to differentiate thus defining for the first time the SRS as it occurs in the adult retina. This differentiation occurs in a posterior-to-peripheral gradient as does the later appearance of interphotoreceptor retinoid-binding protein and photoreceptor outer segments within the SRS (Johnson et al., 1985).

According to Mann (1969), the single row of cone precursors described here represents the earliest recognizable sign of macular differentiation. Although final differentiation of this important area of the retina occurs much later (Mann, 1969;

Hendrickson & Youdelis, 1984; Youdelis & Hendrickson, 1986), it appears that major cellular events, including the compartmentalization of the photoreceptor cells, the formation of synaptic connections, the differentiation of Müller cells and certain second-order neurons, and of the RPE apical surface begin as early as the middle of the third gestational month.

Acknowledgments

The fetal tissue used in this study was collected while the authors were at the Wilmer Institute, the Johns Hopkins University School of Medicine. They would like to thank Drs. Kenneth R. Kenyon, William Richard Green, and John E. Dowling for making the study possible. They are grateful to Dr. Page Erickson for helpful comments on the manuscript, and especially for the light micrographs. This research was supported by National Eye Institute Grant EY00888.

References

Anderson, D.H. & Fisher, S.K. (1979). The relationship of primate foveal cones to the pigment epithelium. *Journal of Ultrastructure Research* **67**, 23–32.

Barber, A.N. (1955). *Embryology of the Human Eye.* St. Louis, Missouri: Mosby.

Blanks, J.C., Adinolfi, A.M. & Lolley, R.N. (1974). Synaptogenesis in the photoreceptor terminal of the mouse retina. *Journal of Comparative Neurology* **156**, 81–94.

Burnside, B. & Laties, A.M. (1976). Actin filaments in apical projections of the primate pigmented epithelial cell. *Investigative Ophthalmology* **15**, 570–575.

Cohen, A.I. (1963). The fine structure of the visual receptors of the pigeon. *Experimental Eye Research* **2**, 88–97.

Dowling, J.E. & Boycott, B.B. (1966). Organization of the primate retina: electron microscopy. *Proceedings of the Royal Society B* (London) **166**, 80–111.

Duke-Elder, S. & Cook, C. (1963). In *Systems of Ophthalmology. Vol. 3: Normal and Abnormal Development, Part I—Embryology*, ed. Duke-Elder, S., London: Kimpton.

Fisher, S.K. & Goldman, K. (1975). Subsurface cisterns in the vertebrate retina. *Cell and Tissue Research* **164**, 473–480.

Fisher, S.K. & Linberg, K.A. (1975). Intercellular junctions in the early human embryonic retina. *Journal of Ultrastructure Research* **51**, 69–78.

Fisher, S.K. & Steinberg, R.H. (1982). Origin and organization of pigment epithelial apical projections to cones in cat retina. *Journal of Comparative Neurology* **206**, 131–145.

Greiner, J.V. & Weidman, T.A. (1980). Histogenesis of the cat retina. *Experimental Eye Research* **30**, 439–453.

Hendrickson, A. & Kupfer, C. (1976). The histogenesis of the fovea in the macaque monkey. *Investigative Ophthalmology* **15**, 746–756.

Hendrickson, A.E. & Youdelis, C. (1984). The morphological development of the human fovea. *Ophthalmology* **91**, 603–612.

Hervouët, F. (1958). Développement normal de l'oeil et de ses annexes, I: Embryologie de la rétine. In *L'Embryologie de L'Oeil et sa Tératologie*, Chapter 3, ed. Dejean, C., Hervouët, F. & Leplat, G., pp. 53–170. Paris, France: Masson & Cie.

Hollenberg, M.J. & Spira, A.W. (1972). Early development of the human retina. *Canadian Journal of Ophthalmology* **7**, 421–491.

Hollenberg, M.J. & Spira, A.W. (1973). Human retinal development: ultrastructure of the outer retina. *American Journal of Anatomy* **137**, 357–386.

Johnson, A.T., Kretzer, F.L., Hittner, H.M., Glazebrook, P.A., Bridges, C.D.B. & Lam, D.M.K. (1985). Development of the subretinal space in the preterm human eye: ultrastructural and immunocytochemical studies. *Journal of Comparative Neurology* **233**, 497–505.

Linberg, K.A. & Fisher, S.K. (1986). An ultrastructural study of interplexiform cell synapses in the human retina. *Journal of Comparative Neurology* **243**, 561–576.

Mann, I. (1969). *The Development of the Human Eye*, 3rd edition, New York: Grune and Stratton.

McArdle, C.B., Dowling, J.E. & Masland, R.H. (1977). Development of outer segments and synapses in the rabbit retina. *Journal of Comparative Neurology* **175**, 253-273.

Missotten, L. (1965). *The Ultrastructure of the Human Retina.* Bruxelles: Editions Arscia S.A.

Mund, M.L. & Rodrigues, M.M. (1979). Embryology of the human retinal pigment epithelium. In *The Retinal Pigment Epithelium*, ed. Zinn, K.M. & Marmor, M.F., pp. 45–54. Cambridge, Massachusetts: Harvard University Press.

Murray, R.L. & Dubin, M.W. (1975). The occurrence of actin-like filaments in association with migrating pigment granules in frog retinal pigment epithelium. *Journal of Cell Biology* **64**, 705–710.

Nir, I., Cohen, D. & Papermaster, D.S. (1984). Immunocytochemical localization of opsin in the cell membrane of developing rat retinal photoreceptors. *Journal of Cell Biology* **98**, 1788–1795.

Olney, J.W. (1968). An electron-microscopic study of synapse formation, receptor outer segment development, and other aspects of developing mouse retina. *Investigative Ophthalmology* **7**, 250–268.

O'Rahilly, R. (1966). The early development of the eye in staged human embryos. *Contributions to Embryology (Carnegie Institution)* **38**, 1–42.

O'Rahilly, R. (1975). The prenatal development of the human eye. *Experimental Eye Research* **21**, 93–112.

Patten, B.M. (1953). *Human Embryology*. New York: McGraw-Hill.

Pfeffer, B.A. & Fisher, S.K. (1981). Development of retinal pigment epithelial surface structures ensheathing cone outer segments in the cat. *Journal of Ultrastructure Research* **76**, 158–172.

Polyak, S.L. (1941). *The Retina.* Chicago: University of Chicago Press.

Provis, J.M., van Driel, D., Billson, F.A. & Russell, P. (1985). Development of the human retina: patterns of cell distribution and redistribution in the ganglion cell layer. *Journal of Comparative Neurology* **233**, 429–451.

Purves, D. & Lichtman, J.W. (1985). *Principles of Neural Development*. Sunderland, Massachusetts: Sinauer Associates, p. 149.

Rhodes, R.H. (1979). A light-microscopic study of the developing human neural retina. *American Journal of Anatomy* **154**, 196–210.

Rhodes, R.H. (1984). Ultrastructure of Müller cells in the developing human retina. *Graefe's Archive for Clinical and Experimental Ophthalmology* **221**, 171–178.

Smelser, G.K., Ozanics, V., Rayborn, M. & Sagun, D. (1974). Retinal synaptogenesis in the primate. *Investigative Ophthalmology* **13**, 340–361.

Spira, A.W. (1975). *In utero* development and maturation of the retina of a non-primate mammal: a light- and electron-microscopic study of the guinea pig. *Anatomy and Embryology* **146**, 279–300.

Spira, A.W. & Hollenberg, M.J. (1973). Human retinal development: ultrastructure of the inner retinal layers. *Developmental Biology* **31**, 1–21.

Steinberg, R.H. (1986). Research update: report from a workshop on cell biology of retinal detachment. *Experimental Eye Research* **43**, 695–706.

Townes-Anderson, E. & Raviola, G. (1981). The formation and distribution of intercellular junctions in the rhesus monkey optic cup: the early development of the cilio-iridic and sensory retinas. *Developmental Biology* **85**, 209–232.

Vogel, M. (1978). Postnatal development of the cat's retina. *Advances in Anatomy Embryology and Cell Biology* **54**, 1–66.

Vrabec, F. (1983). Early differentiation of the human retina. A neurohistological study. *Graefe's Archive for Clinical and Experimental Ophthalmology* **220**, 47–52.

Weidman, T.A. & Kuwabara, T. (1968). Postnatal development of the rat retina. An electron-microscopic study. *Archives of Ophthalmology* **79**, 470–484.

Yamada, E. & Ishikawa, T. (1965). Some observations on the submicroscopic morphogenesis of the human retina. In *The Structure of the Eye*, II: Symposium. ed. Rohen, J.W., pp. 5–16, Stuttgart: F.K. Schattauer-Verlag.

Youdelis, C. & Hendrickson, A. (1986). A qualitative and quantitative analysis of the human fovea during development. *Vision Research* **26**, 847–855.

Zinn, K.M. & Benjamin-Henkind, J.V. (1979). Anatomy of the human retinal pigment epithelium. In *The Retinal Pigment Epithelium*. ed., Zinn, K.M. & Marmor, M.F., pp. 3–31. Cambridge, Massachusetts: Harvard University Press.